

# Puffin Manual

September 21, 2016

# Contents

<b>1</b>	<b>Introduction</b>	<b>3</b>
<b>2</b>	<b>Analytic Equations Solved by Puffin</b>	<b>7</b>
2.1	3D Magnetic Fields . . . . .	9
2.2	Undulator Ends . . . . .	10
2.3	Natural Undulator Focusing . . . . .	13
2.4	Strong Beam Focusing . . . . .	14
2.5	Auto beam-matching . . . . .	15
2.6	To scale or not to scale? . . . . .	15
2.7	Beam Initialization . . . . .	16
2.7.1	Simple . . . . .	17
2.7.2	Dist input . . . . .	18
2.7.3	Beam input . . . . .	18
2.8	Field Mesh . . . . .	19
2.9	Fixing the Radiation Mesh . . . . .	20
2.10	Lattice Input . . . . .	22
<b>3</b>	<b>Parameters</b>	<b>24</b>
3.1	Main Input File . . . . .	24
3.2	Beam Input File . . . . .	31

# 1 Introduction

Puffin (Parallel Unaveraged Fel INtegrator) simulates a Free Electron Laser (FEL). Puffin is a massively parallel numerical solver for an unaveraged, 3D FEL system of equations, and is written mostly in Fortran 90, using MPI and OpenMP.

The initial publication describing the first version of the code is in [1]. The code has undergone many improvements and extended its functionality since then. It no longer uses an external linear solver package, and the only external package now required is FFTW v2.1.5.

Puffin is a so-called 'unaveraged' FEL code - meaning it is absent of the slowly varying envelope approximation (SVEA) and wiggler period averaging approximations. It does not utilize a 'slicing' model of the beam phase space and radiation field, and instead utilizes an algorithm which is much more similar to a Particle-In-Cell (PIC) code methodology.

In addition, some accelerator components are included for simulation of the 'realistic' undulator line, and together with the lack of restrictions, means it may model:

- The full, broad bandwidth frequency spectrum, limited only by the Niquist frequency of the mesh
- Full electron beam transport
- Transport of large energy spread beams through the undulator, and the radiation emitted from these beams
- Tapered undulators
- Fully 3D undulators, including modelling of the wiggler entries/exits and natural focusing
- Interleaved undulator-chicane lattices

- Variably polarized undulators
- Undulator tuning of each module

It presently does not include the effects of space charge, and ignores emission of the backwards wave from the e-beam.

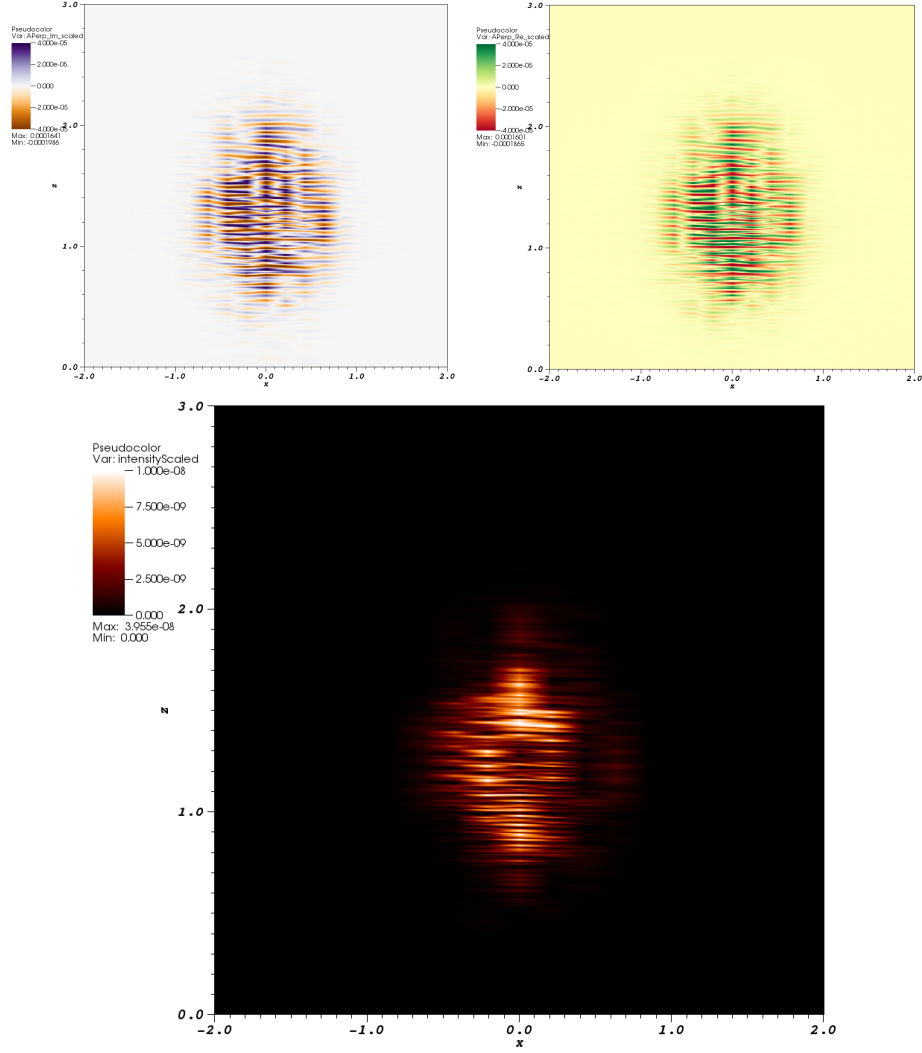


Figure 1: Radiated spontaneous field from Puffin in the first few undulator periods -  $x$  (top left) and  $y$  (top right) polarized fields, and instantaneous intensity (bottom), at  $y = 0$ . Radiation is propagating in the negative  $z$  direction (the vertical axis). One can see the noisy phase of the radiation in both transverse ( $x$ ) and temporal ( $z$ ) directions, which is due to the shot-noise of the electron beam.

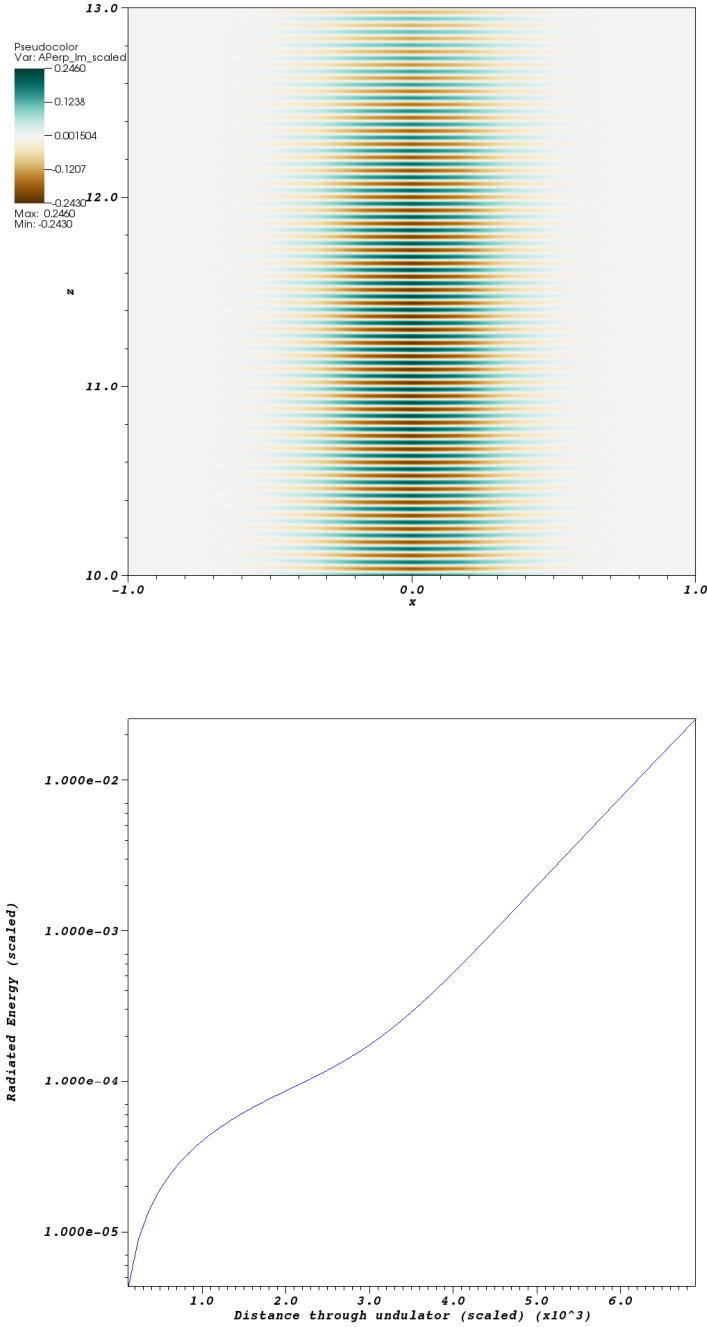


Figure 2: Radiated field from Puffin after amplification in the undulator - x polarized field (top). Radiated energy vs scaled distance through the undulator is on the bottom. Observe the noise from the previous figure has disappeared; the amplification process cause the electrons to align and radiate in phase.

## 2 Analytic Equations Solved by Puffin

The system of equations solved by Puffin have been altered from those described in [1]. They are now:

$$\left[ \frac{1}{2} \left( \frac{\partial^2}{\partial \bar{x}^2} + \frac{\partial^2}{\partial \bar{y}^2} \right) - \frac{\partial^2}{\partial \bar{z} \partial \bar{z}_2} \right] A_{\perp} = -\frac{1}{\bar{n}_p} \frac{\partial}{\partial \bar{z}_2} \sum_{j=1}^N \frac{\bar{p}_{\perp j}}{\Gamma_j} (1 + \eta p_{2j}) \delta^3(\bar{x}_j, \bar{y}_j, \bar{z}_{2j}) \quad (1)$$

$$\frac{d\bar{p}_{\perp j}}{d\bar{z}} = \frac{1}{2\rho} \left[ i\alpha b_{\perp} - \frac{\eta p_{2j}}{\kappa^2} A_{\perp} \right] - i\kappa \frac{\bar{p}_{\perp j}}{\Gamma_j} (1 + \eta p_{2j}) \alpha b_z \quad (2)$$

$$\frac{d\Gamma_j}{d\bar{z}} = -\rho \frac{(1 + \eta p_{2j})}{\Gamma_j} (\bar{p}_{\perp j} A_{\perp}^* + c.c.) \quad (3)$$

$$\frac{d\bar{z}_{2j}}{d\bar{z}} = p_{2j} \quad (4)$$

$$\frac{d\bar{x}_j}{d\bar{z}} = \frac{2\rho\kappa}{\sqrt{\eta}\Gamma_j} (1 + \eta p_{2j}) \Re(\bar{p}_{\perp j}) \quad (5)$$

$$\frac{d\bar{y}_j}{d\bar{z}} = -\frac{2\rho\kappa}{\sqrt{\eta}\Gamma_j} (1 + \eta p_{2j}) \Im(\bar{p}_{\perp j}). \quad (6)$$

Scaled parameters are:-

$$\begin{aligned} \bar{z}_{2j} &= \frac{ct_j - z}{l_c}, & \bar{z} &= \frac{z}{l_g}, \\ \bar{p}_{\perp} &= \frac{p_{\perp}}{mca_u}, & A_{\perp} &= \frac{e\kappa l_g}{\gamma_0 m c^2} E_{\perp}, \\ (\bar{x}, \bar{y}) &= \frac{(x, y)}{\sqrt{l_g l_c}}, & l_g &= \frac{\lambda_w}{4\pi\rho}, \\ l_c &= \frac{\lambda_r}{4\pi\rho}, & \Gamma_j &= \frac{\gamma_j}{\gamma_0}, \\ \rho &= \frac{1}{\gamma_0} \left( \frac{a_u \omega_p}{4ck_u} \right)^{2/3}, & a_u &= \frac{eB_0}{mck_u}, \\ \kappa &= \frac{a_u}{2\rho\gamma_0}, & b_{\perp} &= b_x - ib_y, \end{aligned}$$

$B_0$  is the peak magnetic field in the wiggler.  $\omega_p = \sqrt{e^2 n_p / \epsilon_0 m}$  is the (non-relativistic) plasma frequency, and  $n_p$  is the peak spatial number density of the electron beam ( $N_e / \delta_x \delta_y \delta_z$ ).  $E_\perp = E_x - iE_y$  are the  $x$  and  $y$  radiation electric field vectors.  $\gamma_0$  is the reference energy (Lorentz factor), which is usually taken as the mean beam energy.

The scaled reference velocity,

$$\eta = \frac{1 - \beta_{zr}}{\beta_{zr}} = \frac{\lambda_r}{\lambda_u} = \frac{l_c}{l_g}, \quad (7)$$

where  $\beta_{zr}$  is some reference velocity scaled to  $c$ , which is sensible (but not, strictly speaking, necessary) to take as the mean longitudinal electron velocity in the wiggler, so that

$$\beta_{zr} = \sqrt{1 - \frac{1}{\gamma_0^2} (1 + \bar{a}_u^2)}, \quad (8)$$

where  $\bar{a}_u$  is the *rms* undulator parameter. This defines the velocity at which the electrons travel in the scaled  $\bar{z}_2$  frame. More generally,  $\eta$  describes an \*ideal\* resonance condition - electrons resonant with wavelength  $\lambda_r$  will travel with velocity  $p_2 = 1$  through the  $\bar{z}_2$  frame.

$p_{2j}$  may be worked out analytically from

$$p_{2j} = \frac{1}{\eta} \left[ \left( 1 - \frac{(1 + a_u^2 |\bar{p}_{\perp j}|^2)}{\gamma_r^2 \Gamma_j^2} \right)^{-1/2} - 1 \right] \quad (9)$$

at each step. It is NOT output from Puffin.

Outputs from Puffin are the scaled radiation field  $A_\perp$ , electron phase space coords  $\bar{x}, \bar{y}, \bar{z}_2, \bar{p}_\perp, \Gamma$ , and scaled distance through the undulator  $\bar{z}$ . The normalized electron weights are in the file NormChiDataFile.dat (normalised to the peak \*spatial\* (3D) density).

Compared to the original Puffin paper [1], now the peak magnetic fields are used to scale the system of eqns (as opposed to the *rms* values used previously). Previously (e.g. as described in [1]), the energy exchange was



modelled through the scaled longitudinal velocity  $p_2$ . This was problematic in multiple ways from a computational point of view, since  $p_2$  is a function of the energy,  $p_x$  and  $p_y$ , so that the same quantity was essentially being calculated twice, leading to large errors in some cases. The energy exchange is instead now modelled directly through the scaled variable  $\Gamma_j = \gamma_j/\gamma_r$ , meaning smaller numerical errors and enabling a significantly larger step size.

The formalism for including a variation in the magnetic undulator field, so that  $B_0(\bar{z})$  now varies, was included in [2], and is varied using the parameter  $\alpha(\bar{z}) = \frac{B_0(\bar{z})}{B_0(\bar{z}=0)}$ .

In the most basic form, the input requires 3 files - a ‘main’ input file for parameters, numerical integration, and description of the field mesh, a ‘beam’ input file describing the electron beam, and a ‘seed’ input file describing the radiation seed. Optionally, a lattice file can be used to setup an undulator lattice, including quads, chicanes, and drifts.

## 2.1 3D Magnetic Fields

The undulator is modelled analytically, and the model must include the fast wiggle motion. Puffin may be modified in the future to allow a map of the undulator field to be input. For now, there are a few generic undulator models employed. The magnetic fields available for use in Puffin are the helical, plane-pole, and canted-pole undulator fields discussed in [3], which in the scaled notation here are:-

**helical**

$$b_x = \cos(\bar{z}/2\rho) \tag{10}$$

$$b_y = \sin(\bar{z}/2\rho) \tag{11}$$

$$b_z = \frac{\sqrt{\eta}}{2\rho}(-\bar{x} \sin(\bar{z}/(2\rho)) + \bar{y} \cos(\bar{z}/(2\rho))) \tag{12}$$

### plane-pole

$$b_x = 0 \quad (13)$$

$$b_y = \cosh((\sqrt{\eta}/2\rho)\bar{y}) \sin(\bar{z}/2\rho) \quad (14)$$

$$b_z = \sinh((\sqrt{\eta}/2\rho)\bar{y}) \cos(\bar{z}/2\rho) \quad (15)$$

### canted-pole

$$b_x = \frac{\bar{k}_{\beta x}}{\bar{k}_{\beta y}} \sinh(\bar{k}_{\beta x}\bar{x}) \sinh(\bar{k}_{\beta y}\bar{y}) \sin(\bar{z}/2\rho) \quad (16)$$

$$b_y = \cosh(\bar{k}_{\beta x}\bar{x}) \cosh(\bar{k}_{\beta y}\bar{y}) \sin(\bar{z}/2\rho) \quad (17)$$

$$b_z = \frac{\sqrt{\eta}}{2\rho\bar{k}_{\beta x}} \cosh(\bar{k}_{\beta x}\bar{x}) \sinh(\bar{k}_{\beta y}\bar{y}) \cos(\bar{z}/2\rho) \quad (18)$$

### variably polarized elliptical

$$b_x = u_x \cos(\bar{z}/2\rho) \quad (19)$$

$$b_y = u_y \sin(\bar{z}/2\rho) \quad (20)$$

$$b_z = \frac{\sqrt{\eta}}{2\rho} (u_x \bar{x} \sin(\bar{z}/(2\rho)) + u_y \bar{y} \cos(\bar{z}/(2\rho))) \quad (21)$$

In the 1D approximation,  $b_z = 0$ .

All of the above have an associated ‘natural’ focusing channel, which arises from the off-axis variation in the magnetic fields. This motion arises naturally when numerically solving the equations, and is not superimposed upon the electron motion.

## 2.2 Undulator Ends

The undulators also include entry and exit tapers, and they may be switched on or off in the input file with the flag **qUndEnds**. Setting this to true will model a smooth taper up and down of the undulator magnetic fields in the first and last 2 periods of the undulator, taking the form of a  $\cos^2$ . If

they are switched off, the beam is artificially initialized with an ‘expected’ initial condition in the transverse coordinates for that undulator. Including these ends will model a more realistic and natural entry and exit from the undulator, and will reduce CSE effects from the shape of the wiggler.

The precise description of the undulator ends are as follows. Note the presence of corrective terms in addition to the main  $\cos^2$  term, which ensure the beam oscillates close to the axis. (Note also the very small non-zero initial  $z$ -magnetic field in each case, which we find has no noticable deleterious effects in practice.)

### **Helical Front**

$$b_x = \frac{1}{4} \sin(\bar{z}/16\rho) \cos(\bar{z}/16\rho) \sin(\bar{z}/2\rho) + \sin^2(\bar{z}/16\rho) \cos(\bar{z}/2\rho) \quad (22)$$

$$b_y = -\frac{1}{4} \sin(\bar{z}/16\rho) \cos(\bar{z}/16\rho) \cos(\bar{z}/2\rho) + \sin^2(\bar{z}/16\rho) \sin(\bar{z}/2\rho) \quad (23)$$

$$\begin{aligned} b_z = \frac{\sqrt{\eta}}{2\rho} \Big[ & \bar{x} \left( \frac{1}{32} \cos(\bar{z}/8\rho) \sin(\bar{z}/2\rho) + \frac{1}{4} \sin(\bar{z}/8\rho) \cos(\bar{z}/2\rho) \right. \\ & \left. - \sin^2(\bar{z}/16\rho) \sin(\bar{z}/2\rho) \right) \\ & \bar{y} \left( -\frac{1}{32} \cos(\bar{z}/8\rho) \cos(\bar{z}/2\rho) + \frac{1}{4} \sin(\bar{z}/8\rho) \sin(\bar{z}/2\rho) \right. \\ & \left. + \sin^2(\bar{z}/16\rho) \cos(\bar{z}/2\rho) \right) \Big] \quad (24) \end{aligned}$$

### **Helical Back**

$$b_x = -\frac{1}{4} \cos(\bar{z}/16\rho) \sin(\bar{z}/16\rho) \sin(\bar{z}/2\rho) + \cos^2(\bar{z}/16\rho) \cos(\bar{z}/2\rho) \quad (25)$$

$$b_y = \frac{1}{4} \cos(\bar{z}/16\rho) \sin(\bar{z}/16\rho) \cos(\bar{z}/2\rho) + \cos^2(\bar{z}/16\rho) \sin(\bar{z}/2\rho) \quad (26)$$

$$\begin{aligned} b_z = \frac{\sqrt{\eta}}{2\rho} \Big[ & \bar{x} \left( -\frac{1}{32} \cos(\bar{z}/8\rho) \sin(\bar{z}/2\rho) - \frac{1}{4} \sin(\bar{z}/8\rho) \cos(\bar{z}/2\rho) \right. \\ & \left. - \cos^2(\bar{z}/16\rho) \sin(\bar{z}/2\rho) \right) \\ & \bar{y} \left( \frac{1}{32} \cos(\bar{z}/8\rho) \cos(\bar{z}/2\rho) - \frac{1}{4} \sin(\bar{z}/8\rho) \sin(\bar{z}/2\rho) \right. \\ & \left. + \cos^2(\bar{z}/16\rho) \cos(\bar{z}/2\rho) \right) \Big] \quad (27) \end{aligned}$$

### Plane-Pole Front

$$b_x = 0, \quad (28)$$

$$b_y = \cosh(\sqrt{\eta}\bar{y}/2\rho) \left[ -\frac{1}{4} \sin(\bar{z}/16\rho) \cos(\bar{z}/16\rho) \cos(\bar{z}/2\rho) + \sin^2(\bar{z}/16\rho) \sin(\bar{z}/2\rho) \right], \quad (29)$$

$$\begin{aligned} b_z = \sinh(\sqrt{\eta}\bar{y}/2\rho) \Big[ & -\frac{1}{32} \cos(\bar{z}/8\rho) \cos(\bar{z}/2\rho) + \\ & \frac{1}{4} \sin(\bar{z}/8\rho) \sin(\bar{z}/2\rho) + \sin^2(\bar{z}/16\rho) \cos(\bar{z}/2\rho) \Big], \quad (30) \end{aligned}$$

### Plane-Pole Back

$$b_x = 0, \quad (31)$$

$$b_y = \cosh(\sqrt{\eta}\bar{y}/2\rho) \left[ \frac{1}{4} \sin(\bar{z}/16\rho) \cos(\bar{z}/16\rho) \cos(\bar{z}/2\rho) + \cos^2(\bar{z}/16\rho) \sin(\bar{z}/2\rho) \right], \quad (32)$$

$$\begin{aligned} b_z = \sinh(\sqrt{\eta}\bar{y}/2\rho) \Big[ & \frac{1}{32} \cos(\bar{z}/8\rho) \cos(\bar{z}/2\rho) - \\ & \frac{1}{4} \sin(\bar{z}/8\rho) \sin(\bar{z}/2\rho) + \cos^2(\bar{z}/16\rho) \cos(\bar{z}/2\rho) \Big]. \quad (33) \end{aligned}$$

### Curved-Pole Front

$$b_x = \frac{\bar{k}_{\beta x}}{\bar{k}_{\beta y}} \sinh(\bar{k}_{\beta x} \bar{x}) \sinh(\bar{k}_{\beta y} \bar{y}) \left[ -\frac{1}{8} \sin(\bar{z}/8\rho) \cos(\bar{z}/2\rho) + \sin^2(\bar{z}/16\rho) \sin(\bar{z}/2\rho) \right], \quad (34)$$

$$b_y = \cosh(\bar{k}_{\beta x} \bar{x}) \cosh(\bar{k}_{\beta y} \bar{y}) \left[ -\frac{1}{8} \sin(\bar{z}/8\rho) \cos(\bar{z}/2\rho) + \sin^2(\bar{z}/16\rho) \sin(\bar{z}/2\rho) \right], \quad (35)$$

$$b_z = \frac{\sqrt{\eta}}{2\rho \bar{k}_{\beta y}} \cosh(\bar{k}_{\beta x} \bar{x}) \sinh(\bar{k}_{\beta y} \bar{y}) \left[ -\frac{1}{32} \cos(\bar{z}/8\rho) \cos(\bar{z}/2\rho) + \frac{1}{4} \sin(\bar{z}/8\rho) \sin(\bar{z}/2\rho) + \sin^2(\bar{z}/16\rho) \cos(\bar{z}/2\rho) \right]. \quad (36)$$

### Curved-Pole Back

$$b_x = \frac{\bar{k}_{\beta x}}{\bar{k}_{\beta y}} \sinh(\bar{k}_{\beta x} \bar{x}) \sinh(\bar{k}_{\beta y} \bar{y}) \left[ \frac{1}{8} \sin(\bar{z}/8\rho) \cos(\bar{z}/2\rho) + \cos^2(\bar{z}/16\rho) \sin(\bar{z}/2\rho) \right], \quad (37)$$

$$b_y = \cosh(\bar{k}_{\beta x} \bar{x}) \cosh(\bar{k}_{\beta y} \bar{y}) \left[ \frac{1}{8} \sin(\bar{z}/8\rho) \cos(\bar{z}/2\rho) + \cos^2(\bar{z}/16\rho) \sin(\bar{z}/2\rho) \right], \quad (38)$$

$$b_z = \frac{\sqrt{\eta}}{2\rho \bar{k}_{\beta y}} \cosh(\bar{k}_{\beta x} \bar{x}) \sinh(\bar{k}_{\beta y} \bar{y}) \left[ \frac{1}{32} \cos(\bar{z}/8\rho) \cos(\bar{z}/2\rho) - \frac{1}{4} \sin(\bar{z}/8\rho) \sin(\bar{z}/2\rho) + \cos^2(\bar{z}/16\rho) \cos(\bar{z}/2\rho) \right]. \quad (39)$$

## 2.3 Natural Undulator Focusing

Each undulator type has an associated natural focusing wavenumber. In the helical case, the natural betatron wavenumber is

$$\bar{k}_{\beta nx} = \bar{k}_{\beta ny} = \frac{a_w}{2\sqrt{2}\rho\gamma_0}, \quad (40)$$

with  $\gamma_0$  being the average beam energy (and not necessarily  $= \gamma_r$ )

In the planar case,

$$\bar{k}_{\beta ny} = \frac{a_w}{2\sqrt{2}\rho\gamma_0}. \quad (41)$$

In the canted pole case,

$$\bar{k}_{\beta nx,y} = \frac{a_w \bar{k}_{x,y}}{\sqrt{2}\eta\gamma_0}, \quad (42)$$

where  $\bar{k}_{x,y}$  describe the hyperbolic variation in the transverse directions (see eqns (16 - 18)), and must obey

$$\bar{k}_x^2 + \bar{k}_y^2 = \frac{\eta}{4\rho^2} \quad (43)$$

to be physically valid. They determine the focusing strength in the  $\bar{x}$  and  $\bar{y}$  dimensions. For the case of equal focusing, then,

$$\bar{k}_{\beta nx} = \bar{k}_{\beta ny} = \frac{a_w}{4\rho\gamma_0}. \quad (44)$$

## 2.4 Strong Beam Focusing

In addition to the natural focusing channel, a constant, ‘strong’ focussing channel may be utilized, to focus the beam to a smaller transverse area. This is a magnetic field super-imposed upon the wiggler. It may be switched on or off with the flag **qFocussing** in the main input file, and is specified through the use of the variables **sKBetaXSF** and **sKBetaYSF**. It is probably highly artificial - it may be thought of as physically similar to an ion channel. Nevertheless it allows one to obtain strong focusing without using a lattice. It is defined very simply as

$$b_x = \sqrt{\eta} \frac{\bar{k}_{\beta y}^2}{\kappa} \bar{y}_j, \quad (45)$$

$$b_y = -\sqrt{\eta} \frac{\bar{k}_{\beta x}^2}{\kappa} \bar{x}_j \quad (46)$$

If either **sKBetaXSF** or **sKBetaYSF** are not specified, then no focusing channel will be added for that dimension, even if the **qFocussing** flag is true.

Magnetic quads will be added soon.

## 2.5 Auto beam-matching

The beam, when specified by the ‘simple’ method (see below) may be matched to the focusing channel automatically with the flag **qMatched\_A** in the beam file - the option can be set for each beam. In the scaled notation,

$$\bar{\sigma}_{x,y} = \sqrt{\frac{\rho \bar{\epsilon}_{x,y}}{\bar{k}_{\beta x,y}}} \quad (47)$$

where  $\bar{\epsilon}_{x,y} = \epsilon_{x,y}/(\lambda_r/4\pi)$  are the transverse emittances scaled to the so-called Kim criterion.

The spread in the transverse momentum directions is then given by

$$\bar{\sigma}_{px,py} = \frac{\sqrt{\eta}}{2\kappa} \left\langle \frac{\Gamma}{1 + \eta p_2} \right\rangle \frac{\bar{\epsilon}_{x,y}}{\bar{\sigma}_{x,y}}. \quad (48)$$

where angular brackets indicate the ensemble average of the beam.

If **qFocussing** is true and the strong betatron wavenumber is given, then the strong betatron wavenumber is used to match the beam. Otherwise the beam is auto-matched to the natural focusing channel of the undulator.

## 2.6 To scale or not to scale?

The main algorithm in Puffin utilizes scaled variables to make the numbers ‘nicer’ to work with. The system saturates with scaled intensity  $\sim 1$ , the scaled perpendicular momentum of the beam in the wiggler oscillates between  $-1$  and  $1$ , and so forth. The distance through the wiggler is given in units of a (1D) gain length, and the beam coordinate in the radiation frame is in units of the cooperation length, so that a reference electron slips  $1l_c$  through

Table 1: Input Dimensions and Units for Beam and Radiation Field

Unscaled	units	unscaled equivalent (dimensionless)
$x$	metres (m)	$\bar{x}$
$y$	metres (m)	$\bar{y}$
$dx/dz$	dimensionless	$\bar{p}_x$
$dy/dz$	dimensionless	$\bar{p}_y$
$t$	seconds (s)	$\bar{z}_2$

the radiation field in 1 gain length. The scaling defines a frame of reference which normalises the quantities not only to numerically more manageable numbers, but to *characteristic* variables.

The two dominant variables for the scaling are  $\rho$  and  $\eta$ .  $\eta$  is a function of the wiggler parameters  $a_u$  and  $\lambda_u$ , and reference beam energy  $\gamma_r$ , and is calculated in Puffin from the input. The  $\rho$  parameter is dependent on the peak electron beam number density, amongst other things.

The beam and radiation field parameters may be input in either SI units or the scaled units. Use the variable **qscaled** in the main input file to do this. If = **.true.**, then Puffin expects scaled variables are being used. If SI units are used, then the input parameters will be scaled according to the scaling values specified in the main input file.

Note that they are only *scaling* parameters. The FEL parameter as input does not have to correspond to the beam being input for the results to be correct. The scaled parameters will behave ‘nicely’ if it does, but it is not necessary. When the result is unscaled, the result will still be correct.

## 2.7 Beam Initialization

There are 3 different ways of defining and initializing the electron beam in Puffin:



### 2.7.1 Simple

The beam is described in terms of a homogeneous Gaussian function in every dimension. Some simple correlations in energy can be achieved by specifying an oscillation in the beam energy as a function of  $\bar{z}_2$ , or as a simple linear energy chirp in  $\bar{z}_2$ . The beam is generated in Puffin according to this description.

In general, the correct noise statistics are added to the beam with the method described in [4] (see figure REF). This method, like other noise algorithms, requires a quiet beam to add the noise to. We include two methods of generating the beam - one with the correct noise in all dimensions, and one with the correct noise only in the temporal/ $\bar{z}_2$  dimension. In both methods, the beam is initially quiet in the temporal dimension before adding the noise, with an equispaced layout of the particles in this dimension. The beam MUST be created to appropriately sample the wavelength of emission/amplification - so at least 10 equispaced particles per resonant wavelength. The methods are:-

#### **Equispaced Grid in Every Dimension**

When using this option, the beam is initialized on an equispaced 6D grid. This requires very many particles to appropriately sample every dimension, and you may find it very easy to have more macroparticles than real electrons while loading the beam this way. However, we leave it up to the user to decide if this is appropriate - for some extreme dispersion situation with high charge it may be necessary to create the beam in this way. This can be activated by setting `qEquiXY = true` in the beam input. `qEquiXY` is actually an array of size `nbeams`, with a separate value for each beam if multiple beams are desired. `qEquiXY = false` by default.

#### **Equispaced grid ONLY in $\bar{z}_2$**

If `qEquiXY` is false, then the beam is initially generated as a 1D beam, with equispaced macroparticles. Each macroparticle is then split into many

particles in the other 5 dimensions, with coordinates generated by a quasi-random sequence in each dimension. The SAME SEQUENCE is used for each particle in z2 - the creates a series of beamlets in the  $\bar{z}_2$  dimension, giving a quiet start in  $\bar{z}_2$ . Because random sequences are used, the other 5-dimensions require orders of magnitude less particles to adequately fill the phase space than in the equispaced case. This is the default option, so if not specified, qEquiXY = false.

Both of the above methods may, of course, be replicated and modified by the user to suit a particular situation. The creation of the beam with the correct statistics, while still retaining the sampling necessary for the FEL interaction, is still an area of ongoing research, and is quite controversial. We ultimately leave it to the user to ensure the beam is appropriately initialized for their situation. The methods above can probably be replicated with just a few lines of *e.g.* Python. The generated beam can then be input into Puffin.

To use this, set the option dtype = ‘simple’ in the nblist namelist in the beam file. The parameters for the distribution are then set in the blist namelist in the same file.

### 2.7.2 Dist input

The input is composed of a description of temporal slices along the bunch, describing a Gaussian mean and standard deviation in every other dimension for each temporal slice. This information is used to generate the electron beam in Puffin.

### 2.7.3 Beam input

This method allows one to read in the 6D scaled particle coordinates from a text file. The beam is generated externally. (Arrangement?) The user is

then responsible for the noise in the pulse - it is not added by Puffin in this method.

## 2.8 Field Mesh

The radiation field in Puffin is modelled by a simple cartesian mesh, with equispaced nodes in each of the 3 spatial dimensions. Each node samples a value of the  $x$  and  $y$  polarized radiation field (the  $z$  component of the electric field is not modelled). The scaled  $\bar{z}_2$  coordinate frame is such that the back of the system is with increasing  $\bar{z}_2$  - *i.e.* to the right in figure 3. Recall that  $\bar{z}_2$  is the stationary radiation frame, so that as the beam propagates through the undulator, the beam slips back through the radiation field, moving to the right in figure 3.

This mesh must be large enough to contain the beam through the entire propagation distance through the wiggler.

It must also be large enough to contain the beam in the transverse plane, see figure 4. The radiation field is calculated from the driving electron beam by linear interpolants, so the field must adequately sample the area which the beam occupies. The radiation also diffracts outwards from the beam, so the field mesh must extend to adequately model this diffracting radiation to avoid numerical problems at the boundaries of the grid. There are absorbing boundaries in the outer 16 nodes in the mesh in  $x$  and  $y$  to mitigate this issue, but an absorbing boundary which works well for the full range of frequencies modelled by Puffin is difficult to realise, and the absorbing boundary should not be relied upon to absorb everything which propagates to the outer reaches of the mesh.

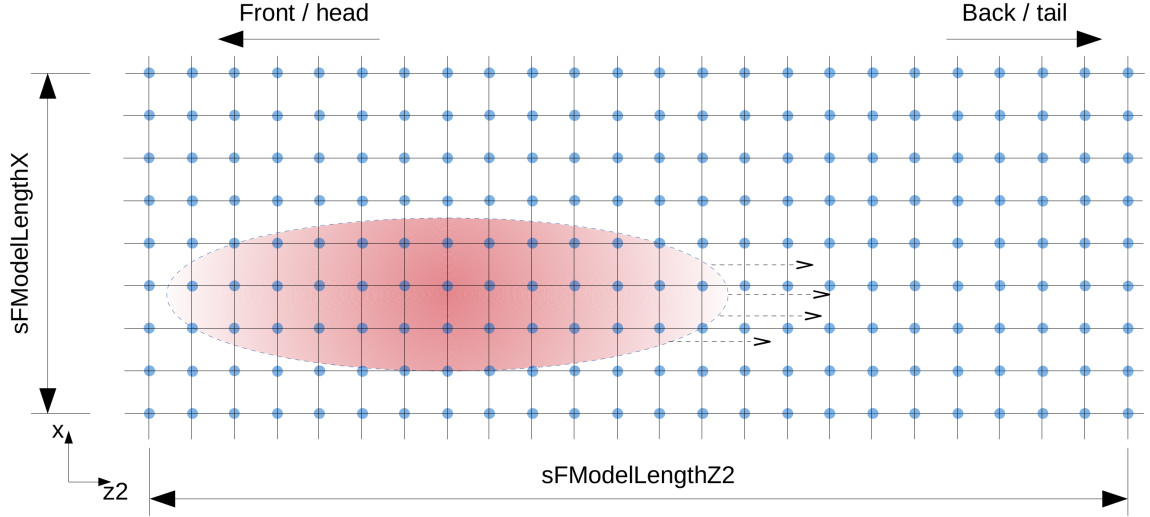


Figure 3: Showing the longitudinal setup of the radiation mesh. The beam is indicated in red. The scaled  $\bar{z}_2$  coordinate is defined so that the front of the radiation and beam is to the left. This is the constant radiation frame, so the beam slips backwards through the field from left to right. In the lab frame, the beam and radiation propagates from right to left. The full length of the mesh must be large enough to contain the beam through propagation.

## 2.9 Fixing the Radiation Mesh

One may use the variables **iRedNodesX**, **iRedNodesY** to fix the mesh around the beam - see figure 4. These variables define an inner set ('reduced' set) of nodes which the beam width will occupy. So the mesh length in  $x$  and  $y$  will be set up such that the inner set of nodes defined by **iRedNodesX**, **iRedNodesY** will contain the beam. In this case, the **sFModelLengthX**, **sFModelLengthY** inputs will be ignored.

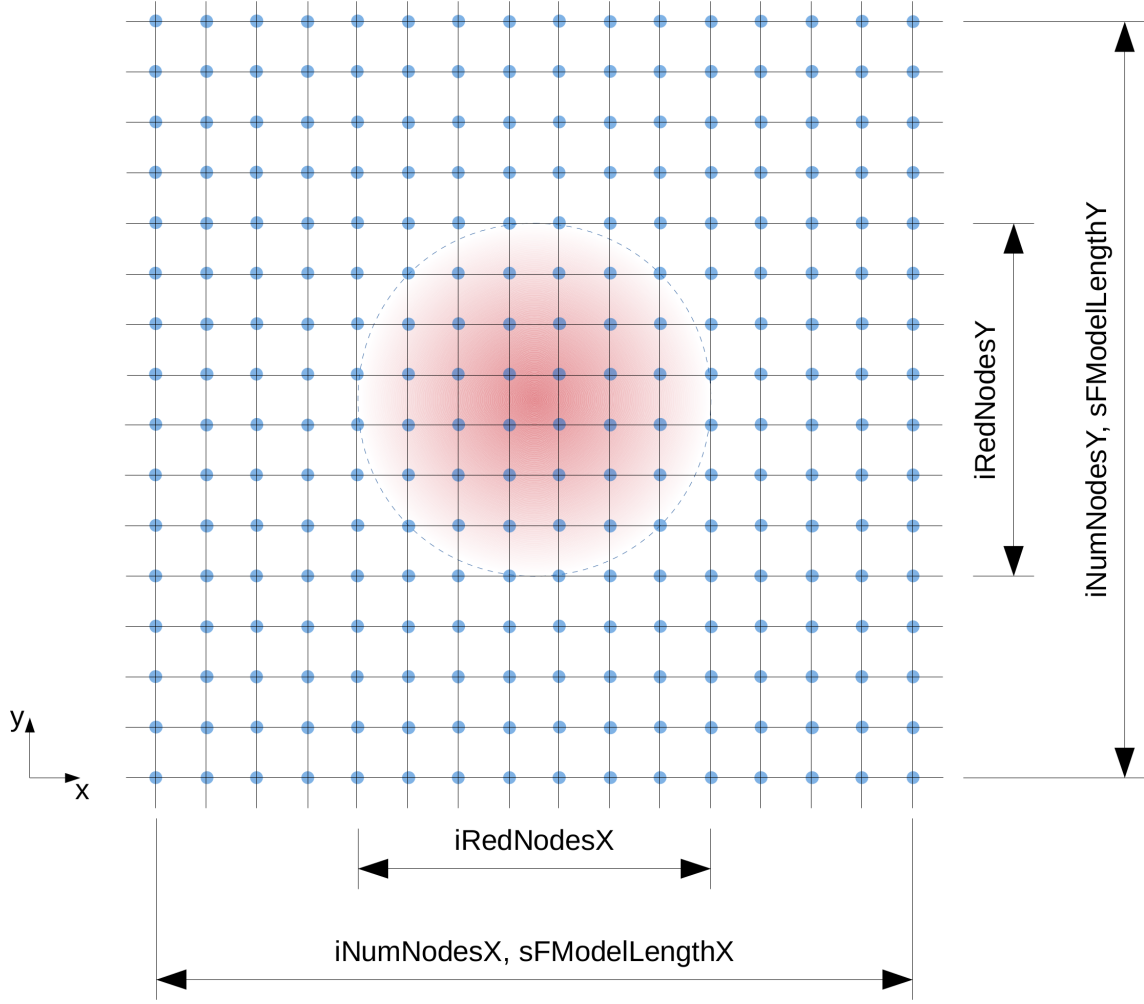


Figure 4: Transverse mesh to model the radiation field - the beam is indicated in red. The mesh may be ‘matched’ to the mesh initially by specifying the  $iRedNodes$  parameters - these specify an inner set of nodes such that the mesh will be setup so that the beam is contained within this number of nodes. This is only an initial condition, but can aid in setting up the mesh.

Table 2: Accelerator components for use in lattice file

Component	ID Initials
Undulator	<b>UN</b>
Quadrupole	<b>QU</b>
Chicane	<b>CH</b>
Drift	<b>DR</b>
Modulation	<b>MO</b>

## 2.10 Lattice Input

A lattice file may be supplied in the main input file with the variable ‘lattFile’. This is the name of the lattice file, containing details of the undulator module lattice layout. If blank, then a single undulator as specified in the main input file will be used.

There are five supported lattice element types, being undulators, quads, chicanes, drifts, and modulations. These are specified in the lattice file by the first 2 characters of each line.

Each entry must be followed by the options specifying that lattice element, on the same line, delimited by spaces.

For the undulator, one must specify the undulator type, the number of wiggler periods  $N_w$ , the undulator parameter relative to the base undulator parameter in the main input file  $\alpha$ , the linear taper  $\frac{d\alpha}{d\bar{z}}$ , the polarization  $u_x$  and  $u_y$  (ignored for the non-variable polarized undulator types), a logical specifying if undulator ends are being used for this module, another logical specifying if a strong focusing channel is being used in the undulator, and the strong focusing strengths  $\bar{k}_{\beta x}$  and  $\bar{k}_{\beta y}$ , and the number of integration steps per period to be used in this module.

For the quad, we must specify  $k$  and  $L$ .

For the chicane, one must specify physical length, slippage length, and dispersion enhancement (R56). The length is the physical length of the device

in undulator periods, and is used to calculate the diffraction properly. The slippage length tells how many wavelengths to delay the beam by relative to the radiation field in resonant radiation wavelengths - be careful, this should not be  $\leq 0$ , or the beam will then be faster than light speed! Similarly, it is left up to the user to decide what is appropriate to delay the beam by with respect to the physical length of the device. The dispersive enhancement is the R56 of the device - using  $\gamma_r$  in the main input as the mean  $\gamma$  for the chicane.

This approach of being able to vary the 3 parameters above is quite flexible, but at the expense of easy automatic checking of the physical relevance of the parameters. For example, one can disperse the beam 'in place', without shifting it w.r.t. the resonant wavelength, which is obviously unphysical. However, this may be useful for a quick setup of the beam for EEHG at the beginning of the undulator, for instance. If one is not sure of the physical length of the actual device, but knows the length between modules and the desired slippage (e.g. for mode locking the FEL), then one can specify the spatial drift between modules using a drift section, and then specify a chicane with zero physical length, but with the desired delay and R56. In this way the radiation diffraction will still be modelled correctly.

For the drift, one must specify length in units of the number of undulator periods.

For the modulation section, one may add an energy modulation to the beam specified by  $\bar{k}_M = \frac{2\pi}{\bar{\lambda}_M}$  and  $\frac{\Delta\gamma}{\gamma_r}$ .

## 3 Parameters

Below is an exhaustive list of parameters, for each filetype. Some options are only really useful for investigating runtime errors or strange behaviour. The parameter list for each file is loosely sorted from most to least useful to the average user.

### 3.1 Main Input File

#### **sRho**

$\rho$ , the FEL parameter. This specifies the scaling of the system. It does **not** have to be strictly correct - it only describes the scaling. The simulation can be performed, and the system may be scaled back to SI units using the supplied scripts (NOT SUPPLIED YET!!). If it is correct, however (meaning, it has been calculated from the beam and undulator parameters input), then the scaled notation becomes physically relevant. For an ideal, 1D system, the system should saturate at intensity  $|A|^2 \approx 1$ , and the system should be firmly in the high or exponential gain regime at  $\bar{z} \approx 2 - 3$ . This allows one to see how efficiently the system is lasing w.r.t its ideal case.

#### **saw**

$a_u$ , the undulator parameter defined with the peak on-axis magnetic field.

#### **sgamma\_r**

$\gamma_0$ , the reference (usually the mean) beam energy.

#### **lambda\_w**

$\lambda_u$ , the undulator, or wiggler, period.

#### **zundType**

Allows one to select from a choice of undulators. Choices are ‘curved’, ‘planepole’, and ‘helical’, described analytically below. If neither of these are chosen, then the default elliptical undulator is chosen, with polarization specified by  $u_x$  and  $u_y$ .



**sux, suy**

$u_x$  and  $u_y$  - the relative peak magnetic field of the undulator in each transverse polarization. Usually, at least one should be = 1, and the other between 0 (planar) and 1 (helical). If they are not defined, the default is helical,  $u_x = u_y = 1$ . Ignored if the undulator type is specified as either ‘helical’, ‘planepole’ or ‘curvedpole’.

**taper**

Taper in the single, simple undulator case,  $\frac{d\alpha}{d\tilde{z}}$ . Ignored if a lattice file is supplied.

**iWriteNthSteps**

Steps at which to write the full data dumps at. This sets the periodicity of the data dumps, in integration steps.

**iWriteIntNthSteps**

Steps at which to write the integrated data at. This sets the periodicity of the writes, in integration steps.

**sFiltFrac**

During the field diffraction step, the lower frequencies are filtered out. This sets the cutoff for the high-pass filter, in units of the reference resonant frequency - (so should usually be  $\leq 0.3$ ).

**sDiffFrac**

Length of the diffraction step, in units of the undulator period. Usually = 1.

**sBeta**

Absorption coefficient for the absorbing boundaries on the transverse grid.

**qOneD**

Logical. If **.true.**, Puffin will be run in 1D mode. Default is **.true.**, since this is the least computationally expensive option.

**qFieldEvolve**

Logical. If = **.false.**, then the radiation field evolution will be switched

off. This is obviously artificial and very rarely used, but can be useful for debugging in some instances. Default is = **.true.**

#### **qElectronsEvolve**

Logical. If = **.false.**, then the electron equations are not solved in the integration steps. Like when qFieldEvolve= **.false.**, this is obviously artificial and very rarely used, but can be useful for debugging in some instances. Default is = **.true.**.

#### **qElectronFieldCoupling**

Logical. If = **.false.**, then the radiation field feedback onto the electrons is switched off by setting the field terms in the electron evolution equations = 0, and so switches off the amplification of the radiation from the electrons. This is unphysical, but is used more often than when qFieldEvolve and qElectronsEvolve = **.false.** . It can often be used to check for gain in the FEL in low gain situations, or to check whether amplification has occurred rather than coherent emission (CSE) effects due to *e.g.* fine structure in the beam. When = **.false.**, this will give the purely spontaneous emission (coherent or incoherent) from the electrons in the wiggler. If there is no appreciable difference between the qElectronFieldCoupling=true and false cases, then there has been negligible FEL amplification.

#### **qSeparateFiles**

If each rank is writing its own file for the hdf5 files. If = true, then the files will need to be gathered together in post for analysis. Depending on the file system, this may be faster or slower.

#### **qFocussing**

Allows one to switch the strong focussing channel on or off. If =bf **.true.**, the strong focusing is switched on with values specified by sKBetaXSF and sKBetaYSF. If qFocussing= **.true.**, yet no focussing strength is specified (sKBetaXSF or sKBetaYSF), then strong focusing is effectively switched off in that dimension. Default = **.false.**.

### **qDiffraction**

Switches modelling of diffraction of the radiation field on or off. If `=.true.`, field diffraction is modelled. This can be useful to switch off only really for debugging purposes. Default `=.true.`.

### **qFMesh\_G**

Whether fixing the field mesh in the transverse plane to contain the beam within the inner `iRedNodesX`  $\times$  `iRedNodesY` nodes.

### **sKBetaXSF, sKBetaYSF**

Betatron wavenumber for energy  $\gamma_r$  of the applied strong focussing channel over the wiggler. Ignored if `qFocussing` is `.false.`. Both = 0 if not specified. Remember this will be applied on top of wiggler field, which has it's own natural focussing.

### **nodesPerLambdar**

Number of nodes in the field mesh to use in the longitudinal dimension per reference resonant wavelength. The reference resonant wavelength is defined from the reference energy `sgamma_r`, the undulator period `lambda_w` and the base or reference undulator parameter `saw` in the usual way.

### **sFModelLengthZ2**

The full length of the field mesh in the longitudinal or temporal dimension. This must be long enough to contain the entire beam as it propagates through the undulator. It is auto-checked at the start of the simulation for the simple beam case only, and the check is only an estimate.

### **sFModelLengthX, sFModelLengthY**

The full length of the field mesh in the x and y (transverse) dimensions. This must be long enough to contain the entire beam as it propagates through the undulator. It is auto-checked at the start of the simulation for the simple beam case only, and the check is only an estimate.

### **sElectronThreshold**

When using the simple beam generation, any macroparticles generated

with weight below the threshold will be removed. The threshold is defined using this variable, which expresses the threshold as a percentage of the mean particle weight.

**lattFile**

The name of the lattice file, if required. If not required, supply a blank string (enter ‘’).

**nPeriods**

Number of undulator periods in the single (non-lattice) undulator case. If a lattice file is supplied, then this is ignored.

**stepsPerPeriod**

Number of integration steps for the electron beam and field source term per undulator period. Should usually be  $\gtrsim$  **nodesPerLambdar** for a beam with energy and wiggler parameter close to the reference parameters.

**qWriteA, qWriteZ2, qWritePperp, qWriteP2, qWriteX, qWriteY, qWriteZ**

Logicals to switch on/off the writing of field, electron phase space coordinates ( $\bar{z}_2, \bar{p}_\perp, \Gamma, \bar{x}, \bar{y}$ ), and propagation distance, respectively, in the sdds full data dumps.

**beam\_file**

String - name of the electron beam input file.

**seed\_file**

String - name of the radiation seed input file.

**iNumNodesX, iNumNodesY**

Number of nodes in the field mesh in the  $x$  and  $y$  transverse dimensions, respectively.

**iRedNodesX, iRedNodesY**

If **qFixMesh** = **.true.**, then the mesh size in  $x$  and  $y$  will be altered in the initialization stage so that the inner **iRedNodesX**  $\times$  **iRedNodesY** nodes in the transverse plane contain the beam.

**nspinDX, nspinDY**

Inner set of transverse nodes to be used in the MPI process updates, which should contain the full transverse beam - auto-calculated in Puffin if wrong.

**qsdds**

Switch on/off output of particle and field mesh dumps in sdds format.

**qhdf5**

Switch on/off output of particle and field mesh dumps in vizSchema compliant hdf5 format.

**qScaled**

Logical turning on/off the input of scaled units into Puffin. If **.true.**, input is assumed to be in the scaled units.

**qFilter**

Logical turning on/off the filtering of low frequency content during the diffraction step. The high-pass filter cut-off is defined by **sFiltFrac**. If true, the low frequency content is set = 0. If false, the low frequency content is not manipulated/diffracted. Default = true.

**qInitWrLat**

Logical. If true, there will be a full particle and field mesh dump at the end of each undulator module in the lattice.

**qUndEnds**

Switch on/off proper modelling of the wiggler module ends. If true, then the first and last 2 periods of the wiggler will be tapered up/down with a  $\sin^2$  function.

**q\_Noise**

If adding the statistical shot-noise to the beam in the simple beam case. Default = true.

**sRedistLen, iRedistStp**

Parallel tuning parameters, controlling the buffer length needed by each

MPI process, and the number of steps per redistribution stage, respectively.

## **3.2 Beam Input File**

As noted in section 2.7, the electron beam file can take 3 different forms.

## References

- [1] L.T. Campbell and B.W.J. McNeil, Physics of Plasmas **19**, 093119 (2012)
- [2] L T Campbell, B.W.J. McNeil and S. Reiche, New J. Phys. **16** (2014) 103019
- [3] E.T. Scharlemann, in High Gain, High Power FELs (edited by R. Bonifacio *et al* ) (1989)
- [4] B. W. J. McNeil, M. W. Poole, and G. R. M. Robb, Phys. Rev. ST Accel. Beams **6**, 070701 (2003)